



Article

The Functionality of IbpA from *Acholeplasma laidlawii* Is Governed by Dynamic Rearrangement of Its Globular–Fibrillar Quaternary Structure

Liliya S. Chernova^{1,2,3}, Innokentii E. Vishnyakov² , Janek Börner³ , Mikhail I. Bogachev⁴ ,
Kai M. Thormann³ and Airat R. Kayumov^{1,*}

¹ Institute of Fundamental Medicine and Biology, Kazan Federal University, Kremlevskaya 18, 420008 Kazan, Russia; lsch-888@live.com

² Institute of Cytology, Russian Academy of Sciences, Tikhoretsky Ave. 4, 194064 St. Petersburg, Russia; innvish@incras.ru

³ Institute of Microbiology and Molecular Biology, Justus Liebig University, Heinrich-Buff-Ring 26, 35392 Giessen, Germany; janek.boerner@mikro.bio.uni-giessen.de (J.B.); kai.thormann@mikro.bio.uni-giessen.de (K.M.T.)

⁴ Centre for Digital Telecommunication Technologies, St. Petersburg Electrotechnical University, Professora Popova 5, 197376 St. Petersburg, Russia; roge@yandex.ru

* Correspondence: kairatr@yandex.ru

Abstract: Small heat shock proteins (sHSPs) represent a first line of stress defense in many bacteria. The primary function of these molecular chaperones involves preventing irreversible protein denaturation and aggregation. In *Escherichia coli*, fibrillar EclbpA binds unfolded proteins and keeps them in a folding-competent state. Further, its structural homologue EclbpB induces the transition of EclbpA to globules, thereby facilitating the substrate transfer to the HSP70–HSP100 system for refolding. The phytopathogenic *Acholeplasma laidlawii* possesses only a single sHSP, A/IbpA. Here, we demonstrate non-trivial features of the function and regulation of the chaperone-like activity of A/IbpA according to its interaction with other components of the mycoplasma multi-chaperone network. Our results show that the efficiency of the *A. laidlawii* multi-chaperone system is driven with the ability of A/IbpA to form both globular and fibrillar structures, thus combining functions of both IbpA and IbpB when transferring the substrate proteins to the HSP70–HSP100 system. In contrast to EclbpA and EclbpB, A/IbpA appears as an sHSP, in which the competition between the N- and C-terminal domains regulates the shift of the protein quaternary structure between a fibrillar and globular form, thus representing a molecular mechanism of its functional regulation. While the C-terminus of A/IbpA is responsible for fibrils formation and substrate capture, the N-terminus seems to have a similar function to EclbpB through facilitating further substrate protein disaggregation using HSP70. Moreover, our results indicate that prior to the final disaggregation process, A/IbpA can directly transfer the substrate to HSP100, thereby representing an alternative mechanism in the HSP interaction network.

Keywords: *Acholeplasma laidlawii*; heat shock; chaperone; sHSP; IbpA; HSP70; HSP100



Citation: Chernova, L.S.; Vishnyakov, I.E.; Börner, J.; Bogachev, M.I.; Thormann, K.M.; Kayumov, A.R. The Functionality of IbpA from *Acholeplasma laidlawii* Is Governed by Dynamic Rearrangement of Its Globular–Fibrillar Quaternary Structure. *Int. J. Mol. Sci.* **2023**, *24*, 15445. <https://doi.org/10.3390/ijms242015445>

Academic Editor: Irmgard Tegeder

Received: 18 August 2023

Revised: 18 October 2023

Accepted: 20 October 2023

Published: 22 October 2023



Copyright: © 2023 by the authors. Licensee MDPI, Basel, Switzerland. This article is an open access article distributed under the terms and conditions of the Creative Commons Attribution (CC BY) license (<https://creativecommons.org/licenses/by/4.0/>).

1. Introduction

Heat shock proteins (HSPs) play a ubiquitous role in the cell stress response. They protect intracellular proteins from improper folding or aggregation, inhibit signal cascades of apoptosis and preserve intracellular signaling pathways that are necessary for the cell survival [1]. Heat shock proteins are classified by the approximate molecular weights of their subunits as HSP100, HSP90, HSP70, HSP60, HSP40 and the small HSP (sHSP, HSP20) families [2]. Among them, the functional chaperone triad consisting of HSP20, HSP70 and HSP100 is one of the key systems responsible for the reverse protein aggregation in various organisms [3–5].

Small heat shock proteins are ATP-independent and represent the first line of protein defense from aggregation. They bind damaged proteins and prevent their further irreversible aggregation; although, they are not capable of further processing the bound proteins [6]. They keep the damaged proteins in a transition state (folding-competent state), from which they can be renatured into correctly folded forms by ATP-dependent chaperones [7]. Because of their “limited” functionality, they were named also as holdases, unlike foldases, which are responsible for the substrate refolding after stress [8].

Small HSPs are characterized by low molecular weights (12–43 kDa) and exhibit three-domain architecture [9–12]. Their primary structure consists of a conserved α -crystallin domain (ACD) flanked by a flexible N-terminal region (NTR) of variable length and a short C-terminal region (CTR) [13,14]. The ACD is a structurally compact β -sandwich consisting of two antiparallel sheets of three and four β -strands, typically 80–100 amino acids in length [15]. The NTR generally includes the (W/F)(D/F)PF-like motif, which participates in the oligomerization of sHSPs and is required for their chaperone-like activity [16]. The CTR contains the strongly conserved V/IXI/V-motif, which interacts with the ACD of another subunit in the multimer during oligomerization [17–19]. While interacting, the NTR and CTR provide the plasticity of the protein quaternary structure, leading to huge oligomer formation that represents a distinct feature of the sHSPs and provides the basis of their functional activity.

HSP70 is a large ubiquitous family of ATP-dependent molecular chaperones that serve as the central hub of the protein homeostasis system [20–23]. The ATP-dependent HSP70 protein DnaK is generally involved in the folding of nascent proteins, transport of proteins across membranes, reactivation of improperly folded proteins and control of regulatory proteins activity [24]. DnaK consists of the N-terminal nucleotide-binding domain (NBD) responsible for the ATPase activity, connected via a flexible linker with the C-terminal substrate-binding domain (SBD), which binds hydrophobic polypeptide segments that are exposed in unfolded proteins [21,25,26] (see Supplementary Figure S1a). The binding of nucleotides to the N-terminal domain of DnaK allosterically regulates the interaction of its C-terminal domain with substrates: ADP stabilizes the substrate binding, and ATP triggers its release. In vivo, DnaK interacts with two co-chaperones: DnaJ (HSP40) and GrpE (a nucleotide exchange factor, NEF). DnaJ delivers substrates to DnaK and stimulates ATP hydrolysis, thereby stabilizing DnaK–substrate interactions. GrpE catalyzes the replacement of ADP by ATP bound to DnaK and promotes dissociation of the substrate, thus turning HSP70 to a substrate-binding ready state [27]. Most species possess several other co-chaperones (HSP40 family members and NEFs), which allow DnaK to act on a variety of substrates in various conditions [24].

For further solubilization and reactivation of aggregated proteins, DnaK interacts with HSP100 protein ClpB. ClpB was initially identified as a heat shock protein necessary for the optimal growth and survival of *Escherichia coli* cells at high temperatures [28]. Unlike many other members of the Clp family, which form complexes with peptidase subunits and participate in the protein degradation, ClpB is a member of a multi-chaperone system together with DnaK, DnaJ and GrpE [29–34]. The N-terminal domain of ClpB is presumably involved in the substrate uptake from DnaK after DnaJ establishes initial weak contact with the surface of the misfolded protein and transfers a segment of the polypeptide for the interaction with DnaK [35]. ClpB can disaggregate some protein substrates without cooperation with DnaK, although the cooperation of ClpB and DnaK produces the most efficient disaggregation [7,36,37]. Interestingly, the ClpB–DnaK cooperation in protein refolding is species-specific, i.e., ClpB interacts efficiently only with DnaK of the same microorganism [38,39].

The mechanism of the HSP20–HSP70–HSP100 chaperone triad activity is well studied in *E. coli*. Due to the duplication of the original *ibpA* gene, *E. coli* encodes two sHSPs: IbpA (from now on referred to as *EcIbpA*) and IbpB (from now on referred to as *EcIbpB*) [40]. *EcIbpA* and *EcIbpB* exhibit 48% identity of amino acid sequences while influencing the substrate aggregation process in different ways [41]. *EcIbpA* binds denatured proteins,

tightly forming stable fibril-like aggregates, which eventually become inefficient substrates for their disaggregation by DnaK/DnaJ and ClpB. To initiate refolding, *EcIbpA* should be displaced from the outer shell of the sHSP–substrate complex, that in turn is facilitated by *EcIbpB* (Supplementary Figure S2) [40–45].

The phytopathogenic mycoplasma *Acholeplasma laidlawii* contains only a single sHSP encoding gene named *ibpA* (from now on referred to as *AlibpA*) [46,47]. In *AlibpA*, the N-terminus provides the formation of 24-mer globules of *AlibpA* while also behaving as an autoinhibitor and activity regulator of the C-terminus, which in turn is required for the chaperone-like activity and protein oligomerization in the fibrous form [48]. Here, we show that the N-terminus of *AlibpA* exerts the function of *EcIbpB* and facilitates further substrate protein disaggregation using HSP70. Moreover, *AlibpA* seems to directly transfer the substrate to HSP100 prior to the final disaggregation, in marked contrast to the well-described HSP70 from *E. coli*, thereby representing an alternative mechanism in the bacterial HSP interaction network.

2. Results

2.1. *AlibpA* in Active (Substrate-Binding) Form Is Present as Fibrils In Vitro

While *AlibpA* has 18% identity with *EcIbpA* and 20% identity with *EcIbpB* (Supplementary Figure S3A,B), the N-terminal domain appears closer to *EcIbpB* than to *EcIbpA* (25% vs. 18% identity), and the C-terminal domain demonstrates 27% identity with *EcIbpA* and 0% with *EcIbpB* (Supplementary Figure S3C). Previously, we have shown that while the full-length *AlibpA* is present mainly as globules with rare fibrils in vitro, the removal of 12 N-terminal amino acid residuals leads to predominant fibrils formation and higher chaperone-like activity [48]. These facts allowed us to hypothesize that the N-terminal domain of *AlibpA* exerts the function of *IbpB*.

First, we tested whether these structural changes in *AlibpA* depend either on the temperature or on the presence of N-termini. For that, full-length *AlibpA*_{His6} and truncated *AlibpA*ΔN12_{His6} were incubated at different temperatures (4 °C, 30 °C and 42 °C), cross-linked with glutaraldehyde followed by the size-exclusion chromatography performed at 25 °C (Figure 1A,C).

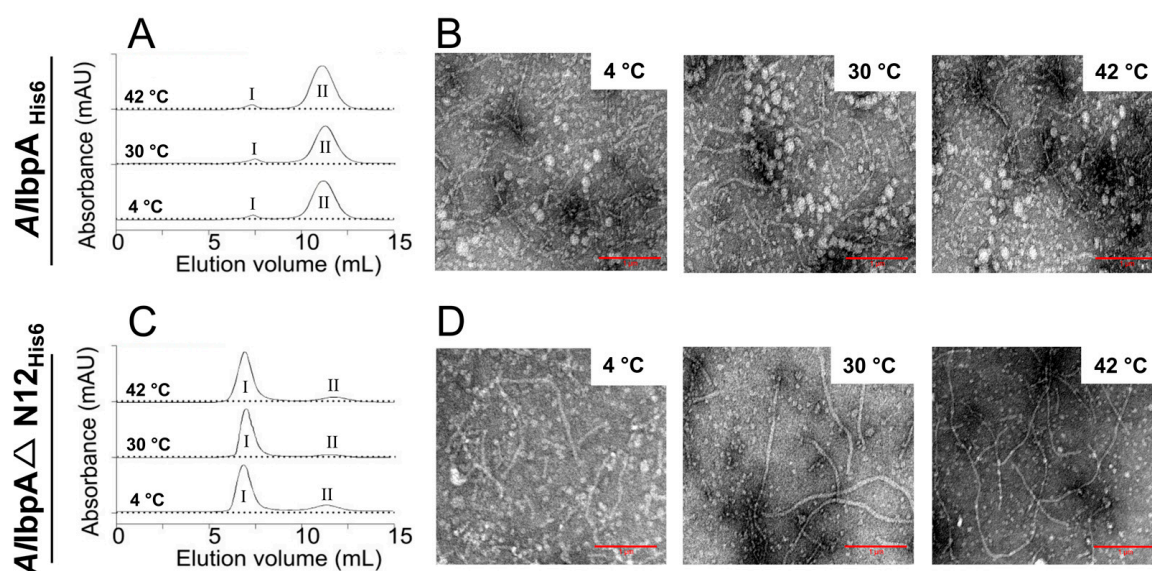


Figure 1. The oligomerization state of recombinant *AlibpA* at various temperatures. The full-length *AlibpA*_{His6} and *AlibpA*ΔN12_{His6} were chemically cross-linked at 4 °C, 30 °C or 42 °C and analyzed with size-exclusion chromatography (A,C) and TEM (B,D). I (first) and II (second) peaks of the elution profile of *AlibpA*_{His6}. The red scale bar at the bottom right corner of each picture indicates the length of 1 μM.

Regardless of the temperature, the full-length *A/lbpA*_{His6} was eluted in two peaks, the minor one at 7.6 mL and the major one at 11.1 mL (Figure 1A), which were earlier shown to correspond to either fibrillar or globular forms of oligomers, respectively [48]. *A/lbpA*ΔN12_{His6} was eluted predominantly as fibrils also independently of the temperature (Figure 1C). Of note, similar elution profiles were observed also for non-cross-linked proteins (Supplementary Figure S4), confirming no cross-linking artifacts. Transmission electron microscopy (TEM) confirmed that the full-length *A/lbpA*_{His6} was the heterogeneous mixture of both globular and fibrous structures (Figure 1B), while *A/lbpA*ΔN12_{His6} was present mostly as fibrils (Figure 1D).

As shown earlier, while being in fibrillar form, *EclbpA* tightly interacts with substrate proteins [41], that is in agreement with higher chaperone-like activity of fibril-forming *A/lbpA*ΔN12_{His6} [48]. Therefore, we next studied whether the fibrillar structure of *A/lbpA*ΔN12_{His6} is retained after the substrate binding or fibrils represent the “storage” form of the protein. For that, *A/lbpA*_{His6} and *A/lbpA*ΔN12_{His6} were mixed with either ADH (alcohol dehydrogenase) or insulin and chemically cross-linked either at 25 °C or at 56 °C, followed by further analysis with TEM (Figures 2 and 3, respectively).

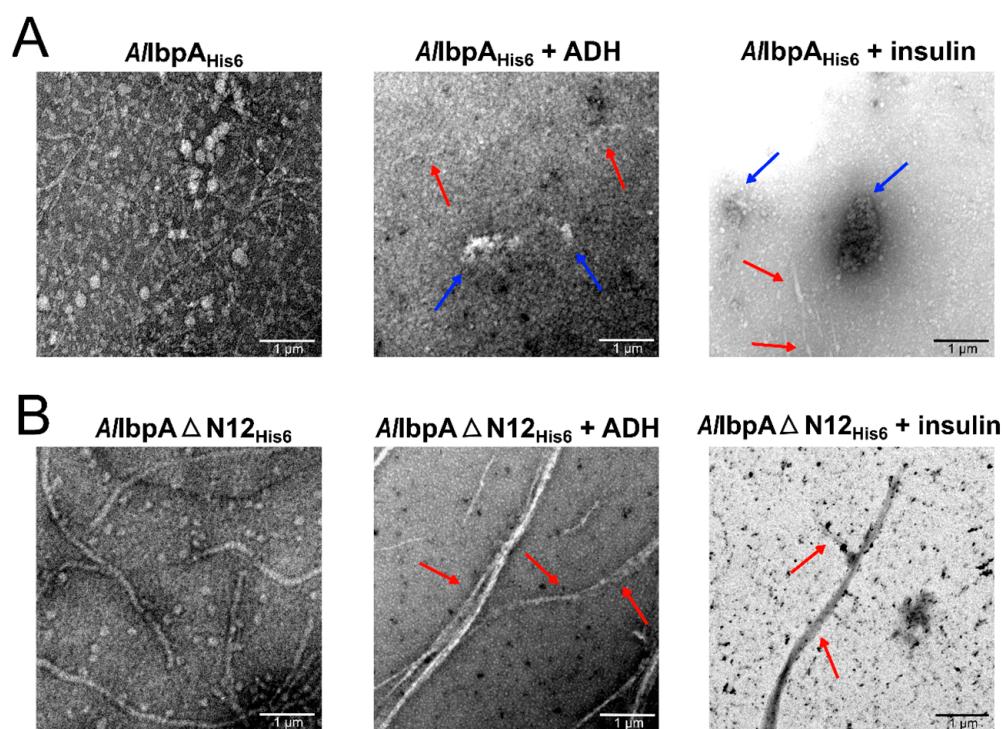


Figure 2. The conformation of oligomers formed by *A/lbpA*_{His6} and *A/lbpA*ΔN12_{His6} in presence of substrate proteins. The full-length (A) or N-terminally truncated (B) *A/lbpA*_{His6} proteins were pre-incubated for 30 min at 25 °C with either ADH (alcohol dehydrogenase) or human insulin, treated with glutaraldehyde and analyzed with TEM. Blue arrows show globular co-aggregates, and red arrows show fibrillar structures. The scale bar at the bottom right corner of each picture indicates the length of 1 μM.

Of note, both insulin and ADH were reported previously as relevant substrates for various HSP20 [49–51], including *A/lbpA* [47,48]. In the presence of substrate proteins, at low temperatures, the full-length *A/lbpA*_{His6} led to the formation of aggregates that appeared as globules up to ten-fold larger compared to solely sHSPs or substrate proteins (Figure 2A and Supplementary Figure S5, respectively). By contrast, the *A/lbpA*ΔN12_{His6} appeared as fibrils and formed fibrillar structures also in the presence of either ADH or insulin (Figure 2B), despite proteins interacting even at 25 °C, as shown earlier in [48].

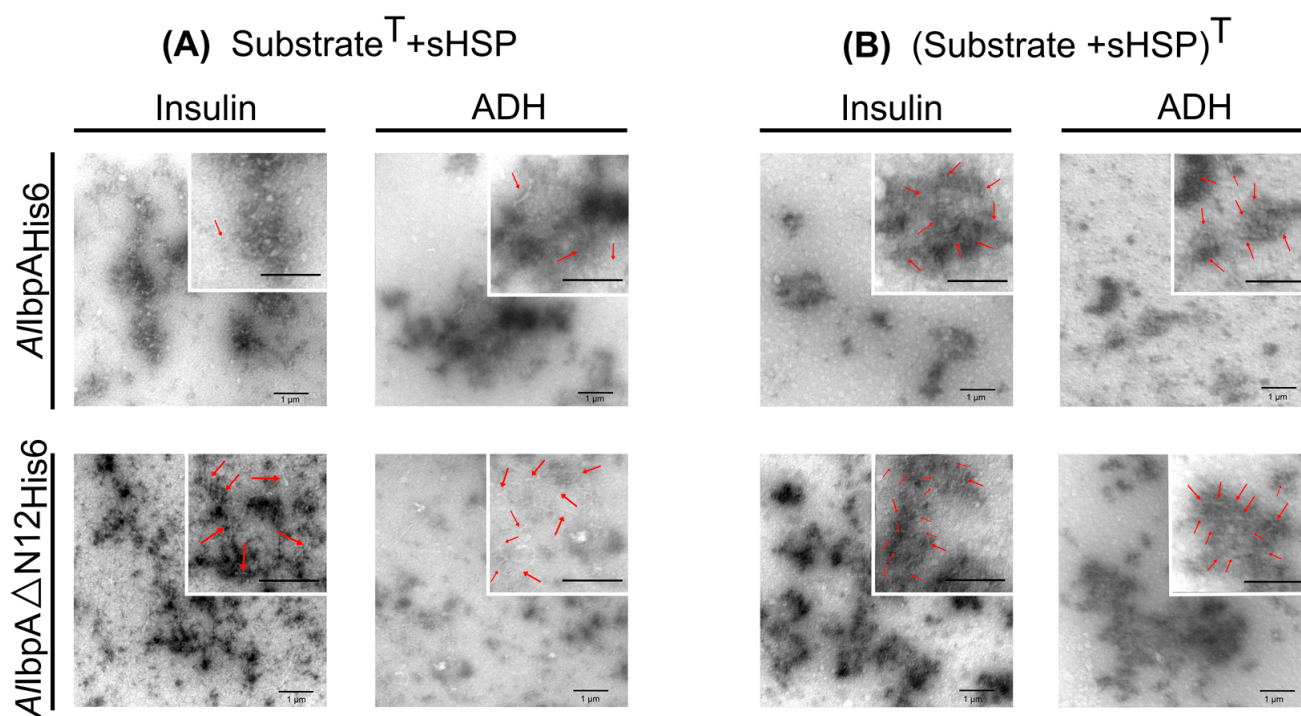


Figure 3. The conformation of oligomers formed by *A/IbpA_{His6}* and *A/IbpAΔN12_{His6}* in presence of substrate proteins under heat-treated alone (A) or in the presence of sHSPs (B). The substrate proteins were pre-incubated for 30 min at 56 °C (indicated as T) with either *A/IbpA_{His6}* or *A/IbpAΔN12_{His6}*, treated with glutaraldehyde and analyzed with TEM. Red arrows show fibrillar structures. The black scale bar at the bottom right corner of each picture indicates the length of 1 μm.

The pre-denaturation of either ADH or insulin at 56 °C resulted in the formation of large aggregates (Supplementary Figure S5), and the addition of sHSPs did not change the size and morphology of substrate aggregates (Figure 3A). Samples with the full-length *A/IbpA_{His6}* were of similar conformation as in the experiment performed at 25 °C, primarily forming globule-like structures around the denatured protein; nevertheless, some fibrils were also found near the substrate proteins (see red arrows). *A/IbpAΔN12_{His6}* was observed in the form of fibrils, although they were shorter compared to the low-temperature experiment (compare Figures 2A and 3A). The heat treatment of substrate proteins in the presence of sHSPs led to a different type of aggregate formation, with the aggregates appearing much smaller in their sizes and being more sparsely represented. A large amount of material appeared as short fibrils (50–100 nm in length) surrounded by a contrast agent for both *A/IbpA_{His6}* and *A/IbpAΔN12_{His6}* (Figure 3B), apparently representing substrate–sHSP complexes.

Taken together, these data suggest that in vitro *A/IbpA_{His6}* transforms from globules to fibrils in the active (substrate-binding) state similarly to *EclpA*.

2.2. *A/IbpA* Interacts with *A/DnaK* and *A/ClpB* In Vitro

To test whether *A/IbpA* interacts with *A/DnaK* and *A/ClpB*, co-elution of recombinant *A/IbpA_{His6}* on Ni-NTA Sepharose was performed. *A/IbpA_{His6}* was pre-incubated with extracts of *A. laidlawii* cells at either optimal (30 °C) or stress conditions (4 °C and 42 °C) and purified. Those proteins that co-eluted with the recombinant *A/IbpA_{His6}* were identified by LC-MS (liquid chromatography–mass spectrometry). In addition to a broad spectrum of other proteins, *A/ClpB* and *A/DnaK* were identified regardless of the incubation temperature (Table 1). However, more HSPs were co-eluted with increasing temperature, as indicated by higher emPAI values at 42 °C.

Table 1. Amount of *A*/ClpB and *A*/DnaK co-eluting with *A*/IbpA from *A. laidlawii* cell crude extract.

	Score			emPAI		
	4 °C	30 °C	42 °C	4 °C	30 °C	42 °C
<i>A</i> /DnaK	465	1508	1412	0.47	0.73	0.83
<i>A</i> /ClpB	222	532	11,703	0.09	0.31	2.72

The alignment of *dnaK* and *clpB* genes from *A. laidlawii* and *E. coli* revealed 54% and 56% identity, respectively (Supplementary Figures S1 and S6), suggesting similarities in the HSP20–HSP70–HSP100 systems functionality in these bacteria.

A/DnaK_{ST} and *A*/ClpB_{ST} were overexpressed in *E. coli*, purified, and the interaction of the recombinant *A*/IbpA_{His6} with *A*/DnaK_{ST} and *A*/ClpB_{ST} was studied in vitro with bio-layer interferometry using the BLItz system (Figure 4). Both *A*/DnaK_{ST} and *A*/ClpB_{ST} were able to interact with *A*/IbpA_{His6} (dissociation constant $K_D = 3.1 \pm 0.3 \mu\text{M}$ and $1.2 \pm 0.2 \mu\text{M}$, respectively), although less efficiently compared to insulin ($K_D = 0.1 \pm 0.02 \mu\text{M}$). Interestingly, the *A*/IbpA_{His6}–*A*/ClpB_{ST} complex became very stable as dissociation was low. The interaction between *A*/DnaK_{ST} and *A*/ClpB_{ST} was weak ($K_D = 20.3 \pm 2.2 \mu\text{M}$), suggesting that these proteins interact preferentially with sHSPs. Furthermore, the interaction of the recombinant *A*/IbpA_{His6} with *A*/DnaK_{ST} or *A*/ClpB_{ST} was confirmed via co-elution on the agarose Ni-NTA column (Supplementary Figure S7).

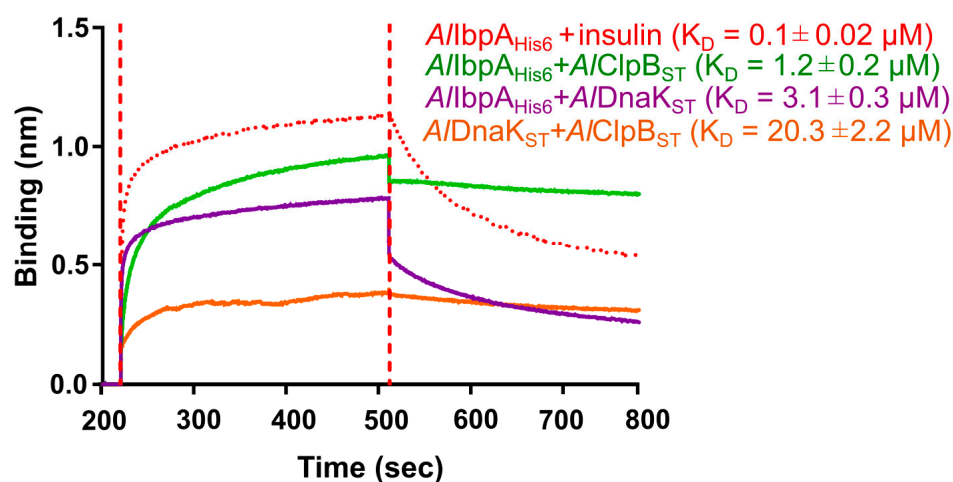


Figure 4. The interferometric analysis of recombinant *A*/IbpA, *A*/ClpB and *A*/DnaK interaction in vitro on the BLItz instrument (FortéBio, Fremont, CA, USA). Either *A*/IbpA_{His6} or *A*/DnaK_{ST} was loaded onto a streptavidin biosensor until 2.0 nm protein was bound to the surface, and after 30 s washing in PBS, the sensor was immersed into either *A*/ClpB_{ST} or *A*/DnaK_{ST} solutions (10 μM). The dissociation constant (K_D) calculation was performed with BLItz Pro data analysis software (version: 1.3.0.5). The interaction of *A*/IbpA with insulin (red dots) served as a positive binding control. The standard deviations are indicated as range behind the calculated mean values of technical triplicates.

2.3. The Impact of *A*/IbpA in Fibrillar Form on Its Interaction with *A*/DnaK and *A*/ClpB and Substrate Transfer to HSPs

It was shown earlier that *Ec*IbpA bound in fibrillar form to the substrate protein impairs the transfer of the latter to DnaK and ClpB [40–45]. Therefore, we studied the impact of *A*/IbpA in fibrillar form for the interaction with *A*/DnaK and *A*/ClpB and substrate transfer to HSPs in vitro and in vivo.

Our results indicate that the affinities of full-length *A*/IbpA_{His6} to the surface-bound *A*/DnaK_{ST} and *A*/ClpB_{ST} were similar to previously reported data ($K_D = 0.1 \mu\text{M}$ and $0.2 \mu\text{M}$, respectively, comparing Figures 4 and 5). The deletion of the N-terminus of *A*/IbpA decreased the binding affinity of *A*/IbpA Δ N12_{His6} to *A*/DnaK_{ST} 15-fold (Figure 5A), suggesting that the fibrillar form of *A*/IbpA impairs its interaction with large HSPs, as shown previously for fibrillar *Ec*IbpA. In contrast, no similar effect could be observed

for *A/ClpB_{ST}*, assuming no significant impact of the *A/IbpA* quaternary structure on the interaction of these proteins.

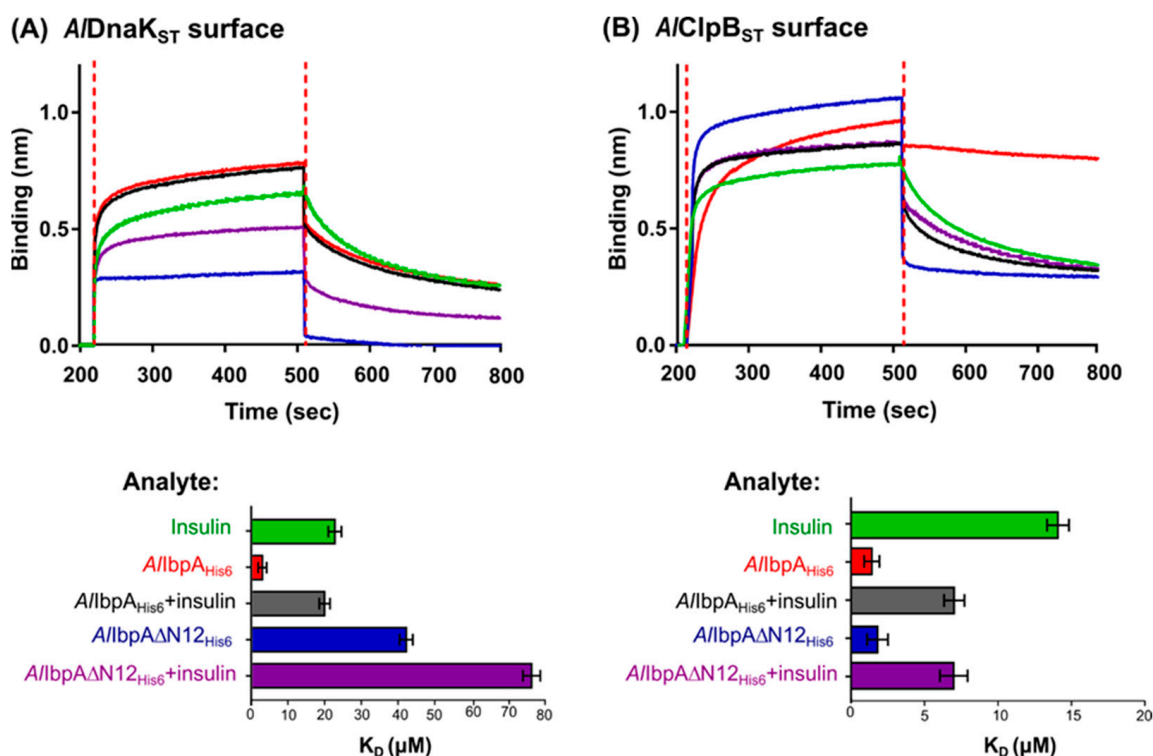


Figure 5. The interferometric analysis of recombinant *A/DnaK* and *A/ClpB* interaction with sHSP-bound substrate in vitro on the BLItz instrument (FortéBio, Fremont, CA, USA). Either *A/DnaK_{ST}* (A) or *A/ClpB_{ST}* (B) was loaded onto streptavidin biosensor until 2.0 nm protein was bound to the surface. After 30 s washing in PBS, the sensor was immersed into recombinant either full-length *A/IbpA_{His6}* or *A/IbpAΔN12_{His6}* solely protein solution or proteins chemically cross-linked with insulin by glutaraldehyde. K_D calculation was performed with BLItz Pro data analysis software (version: 1.3.0.5). The standard deviations of the mean values from technical triplicates are shown as error bars.

Next, the interaction of *A/DnaK* and *A/ClpB* with insulin complexes with either fibrillar or globular forms of *A/IbpA* in sHSP–substrate complexes (as seen in Figure 2) was investigated. For that, either *A/IbpA_{His6}*–insulin or *A/IbpAΔN12_{His6}*–insulin complexes were cross-linked in vitro. Further, their interaction with either *A/ClpB_{ST}* or *A/DnaK_{ST}* immobilized on the sensor was analyzed.

Affinities of both *A/DnaK_{ST}* and *A/ClpB_{ST}* to full-length *A/IbpA_{His6}* bound with insulin increased approximately five-fold compared with solely sHSPs (Figure 5), suggesting that *A/IbpA* dissociation from the complex with substrate protein is required to recruit the latter to bind with the large HSPs, as shown previously in *E. coli* [45]. Of note, only a two-fold increase in K_D was observed for *A/DnaK_{ST}* interaction with insulin-bound *A/IbpAΔN12_{His6}*, suggesting that the fibrillar form of sHSPs appears as the main negative factor affecting the protein interaction. These data suggest that the interaction of *A/IbpA* in fibrillar form with *A/DnaK* is unfavorable, although the interaction with *A/ClpB* does not depend on the sHSP quaternary structure.

Further, the role of both fibrillar and globular forms of oligomeric *A/IbpA* for the cooperation of the latter with HSP70 and HSP100 was evaluated via assessing the ability to prevent the insulin denaturation in vitro. Human insulin was heated in the presence of various combinations of HSP20, HSP70 and HSP100, as indicated in Figure 6, and the melting temperature (T_m) was assessed using SYPRO Orange assay. The T_m values of pure proteins are shown in Supplementary Figure S8.

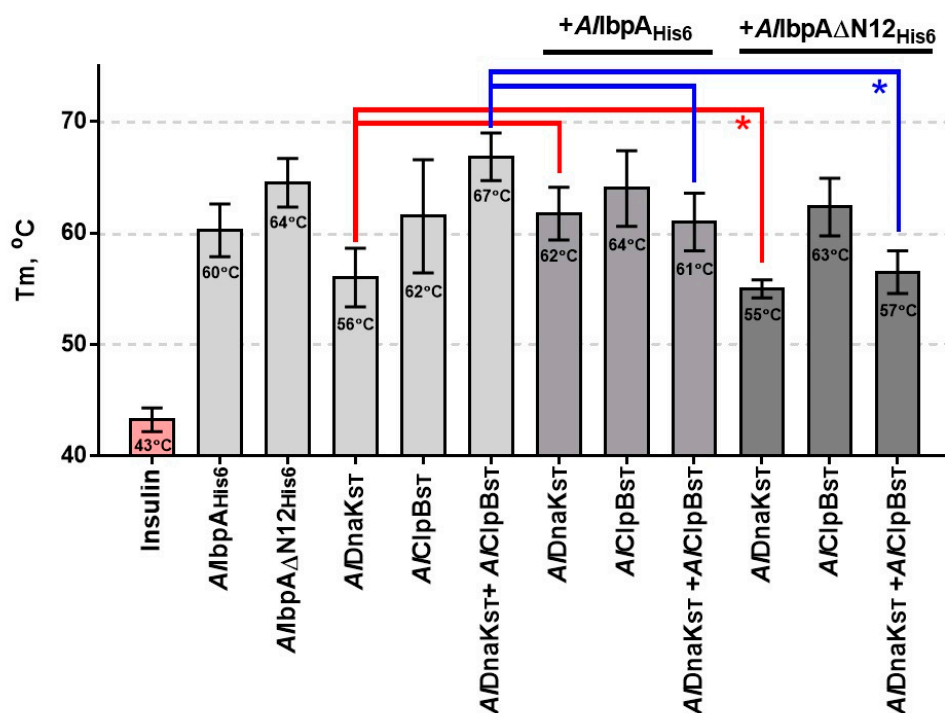


Figure 6. The capacity of recombinant A/HSPs to prevent the temperature-induced denaturation of insulin in vitro. Various recombinant A/HSPs (0.1 mg) were mixed with insulin (0.1 mg) in total volume of 30 μ L and heated from 10 $^{\circ}$ C to 95 $^{\circ}$ C with a temperature increment of 1 $^{\circ}$ C per 1 min in the presence of 10 μ M SYPRO Orange. The fluorescence was detected using FAM filter set detection on Bio-Rad CFX96 thermocycler. The data analysis was performed by determining the temperature leading to fluorescence increase by 100% of maximal signal (T_m). Asterisks show statistically significant differences ($p < 0.05$). Error bars indicate the standard deviation of the mean values from technical triplicates.

Solely insulin was denatured completely at 43 $^{\circ}$ C; whereas, in the presence of either full-length or truncated A/lbpA_{His6}, the T_m increased up to 60 $^{\circ}$ C and 64 $^{\circ}$ C, respectively. A/DnaK_{ST} and A/ClpB_{ST} alone were less efficient in the insulin denaturation prevention (T_m = 56 $^{\circ}$ C and 62 $^{\circ}$ C, respectively) compared to their complex (T_m = 67 $^{\circ}$ C). The combination of A/DnaK_{ST} with A/lbpA_{His6} increased the T_m by 6 $^{\circ}$ C ($p < 0.05$), while A/lbpA Δ N12_{His6} abrogated this effect (see Figure 6 red line). The combination of either A/lbpA_{His6} or A/lbpA Δ N12_{His6} with A/ClpB_{ST} did not affect the T_m. The addition of either A/lbpA_{His6} or A/lbpA Δ N12_{His6} to the A/DnaK_{ST}–A/ClpB_{ST} complex led to T_m to decrease by 6 $^{\circ}$ C and 10 $^{\circ}$ C, respectively. Neither A/lbpA_{His6} nor A/lbpA Δ N12_{His6} affected the T_m of insulin in the presence of A/ClpB_{ST}, which is in agreement with their close binding affinities (see Figure 5B).

2.4. The In Vivo Assessment of the Role of HSP20, HSP70 and HSP100 in Heat Resistance of Cells

The effect of A/lbpA_{His6} and A/lbpA Δ N12_{His6} overexpression on the heat resistance was evaluated in recombinant *E. coli* BL21 cells lacking their own endogenous HSPs. *E. coli* strains carrying pET-A/lbpA_{His6}, pET-A/lbpA Δ N12_{His6} and pET15b empty vector as negative control were induced with the addition of IPTG and after 1 h incubation at 30 $^{\circ}$ C were subjected to heat treatment (56 $^{\circ}$ C) for 1 h. The cellular viability was measured using the MTT test (Figure 7) and expressed as a percentage of the residual metabolic activity of the cells after heating. Additionally, colony forming units (CFUs) were calculated. These data are shown in Supplementary Figure S9.

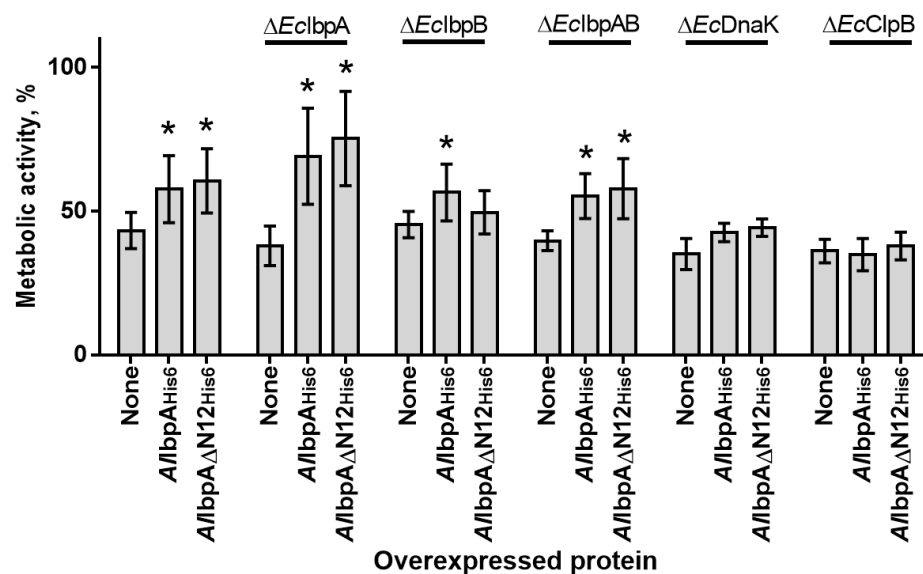


Figure 7. The viability of *E. coli* BL21 and its HSP-deficient derivatives ectopically overexpressing either full-length or N-terminally truncated *AllbpA*. Cells carrying pET15b vector without insert served as a control (marked as “None”). Exponentially growing cells were induced with 1 mM IPTG. After 2 h of growth at 30 °C, cultures were heat-treated (1 h at 56 °C) and residual viability was assessed in MTT assay. Data are present as mean \pm standard deviations of biological triplicates with 3 technical repeats of each. The metabolic activity of cells growing at 37 °C was considered as 100%. Asterisks show statistically significant difference between cell with and without sHSP overexpression ($p < 0.05$). The standard deviations of the mean from biological triplicates are shown as error bars.

The thermotolerance of *E. coli* did not decrease significantly upon deletion of physiological HSPs indicated by comparable residual viability of all strains (40–50%). The heterologous expression of full-length *AllbpA*_{His6} increased the thermotolerance of $\Delta EcIbpA$ and in lesser extent of $\Delta EcIbpB$ and $\Delta EcIbpAB$ cells, while *AllbpA*_{N12His6} affected only $\Delta EcIbpA$ and $\Delta EcIbpAB$ cells. These data suggest that the N-terminus of *AllbpA* is responsible for the same functions as *EcIbpB*. No effect of either *AllbpA*_{His6} or *AllbpA*_{N12His6} on the thermotolerance of $\Delta EcDnaK$ and $\Delta EcClpB$ cells could be observed, suggesting that *AllbpA* could replace own sHSPs of *E. coli* in $\Delta EcIbpA$, $\Delta EcIbpB$ and $\Delta EcIbpAB$ cells.

3. Discussion

HSPs are cellular tools participating in protein quality control by the refolding of misfolded proteins [1]. A functional chaperone triad consisting of HSP20, HSP70 and HSP100 is one of the main systems responsible for the damaged protein refolding [3–5].

Small heat shock proteins bind damaged proteins, prevent their further irreversible aggregation and transfer them to ATP-dependent chaperones that are capable of renaturing them into correctly folded forms [7]. A crucial function of the sHSPs–substrate interaction is keeping the aggregating proteins in a refolding-competent state, which prevents their irreversible denaturation and subsequently allows refolding by HSP70 and HSP100 [7]. The sHSP system of *E. coli*, consisting of the two proteins *EcIbpA* and *EcIbpB*, is still considered the most studied among prokaryotes (Supplementary Figure S2) [40]. In the form of fibril-like oligomers, *EcIbpA* efficiently binds proteins with disrupted conformation. In complex with *EcIbpB*, the fibrillar *EcIbpA* forms globule-like oligomers that can easily transfer the substrate to the next members of the chaperone system by dissociating from the substrate (Supplementary Figure S2a). However, the absence of *EcIbpB* disrupts this process, complicating further interaction of *EcDnaK* with the substrate and thereby inhibiting substrate processing by the multi-chaperone system (Supplementary Figure S2b) [43,44,52].

AllbpA forms in vitro a mixture of fibrillar and globular oligomers suggesting that it possesses the function of both *IbpA* and *IbpB* (Figure 1A,B [48]). The deletion of the

N-terminus of *A*IbpA led to the formation of homogenous fibrillar quaternary protein structure depending neither on the temperature (Figure 1C,D) nor on the substrate binding (Figure 2B). This fact allows for the suggestion that the N-terminus of *A*IbpA could possess the function of *Ec*IbpB from the *E. coli* dual-sHSP system (Supplementary Figure S2). Further, the substrate proteins treated with high temperature (56 °C) in the presence of sHSPs formed complexes, appearing as short fibrils for both *A*IbpA_{His6} and *A*IbpAΔN12_{His6} (Figure 3B). Thus, both fibrillar and globular *A*IbpA_{His6} are capable of dynamically rearranging into short fibrils to exhibit chaperone-like activity towards the aggregating substrate (Figure 3B). Together with higher chaperone-like function of fibrillar *A*IbpAΔN12_{His6} compared to globular *A*IbpA_{His6} (Figure 6, [48]), it is likely that the fibrillar quaternary structure represents the active form of *A*IbpA. Thus, based on the quaternary structure similarities of the N-terminal-truncated *A*IbpA_{His6} (Figure 2B) and *Ec*IbpA [53], we assume that *A*IbpA behaves as *Ec*IbpA, which efficiently binds denatured proteins by forming fibril-like co-aggregates. By contrast, *Ec*IbpA is inefficient for DnaK/DnaJ/GrpE- and ClpB-mediated disaggregation in the absence of *Ec*IbpB because of its inability to transit to globular form and dissociate from the substrate [40,42–45]. Indeed, when insulin was chemically bound to either *A*IbpA_{His6} or *A*IbpAΔN12_{His6}, the interaction of these complexes with both *A*DnaK_{ST} and *A*ClpB_{ST} decreased drastically (Figure 5), probably due to the competitive substitution of sHSPs by large HSPs becoming unavailable. Furthermore, *A*IbpAΔN12_{His6} had 15-fold lower affinity to *A*DnaK_{ST} (Figure 5A), apparently because of its tight binding to insulin in fibrillar form, behaving similar to *Ec*IbpA. Unlike *Ec*ClpB, the interaction of *A*IbpAΔN12_{His6} with *A*ClpB_{ST} was not affected (Figure 5B).

On the other hand, *A*IbpAΔN12_{His6} was not only impaired in binding to *A*DnaK_{ST} (Figure 5A) but also the activity of the entire multi-chaperone system was repressed, as shown by the in vitro chaperone activity assay (Figure 6). A similar effect was described for multi-chaperone activity of *E. coli* in *Ec*IbpB-deficient cells (Supplementary Figure S2B, [41]). Thus, *A*IbpA_{His6} had no influence on in vitro chaperone activity in the presence of one component of the HSP70–HSP100 system (Figure 6). When both HSPs were present, the functionality of this system decreased by the presence of *A*IbpA_{His6} due to incomplete sHSP–substrate complex dissociation. Despite the ability of *A*ClpB_{ST} to interact with the *A*IbpAΔN12_{His6}–substrate complexes (Figure 5B), the presence of *A*DnaK_{ST} seems to inhibit the multi-chaperone activity in vitro, lining up that *A*IbpA interacts with *A*DnaK prior to *A*ClpB (Figure 6).

To evaluate the physiological role of HSP20, HSP70 and HSP100 from *A. laidlawii* in vivo, an artificial recombinant system with *E. coli* BL21 was used, where the *ibpA*, *bpB*, *dnaK* and *clpB* genes were deleted. *E. coli* cells expressing full-length *A*IbpA_{His6} became thermotolerant to high temperature (56 °C), while retaining the growth comparable to that observed at 37 °C (Supplementary Figure S10D), suggesting that *A*IbpA is able to fulfill beneficial functions in the early heat stress response of this organism, as it was already shown when overexpressing native IbpA or IbpB [54]. Remarkably, a similar phenotype was observed for the *dnaK* deletion mutant, expressing *A*IbpA_{His6}, even though the biological triplicates showed higher heterogeneity in the growth behavior. Without *A*IbpA_{His6} overexpression, no growth could be observed at 56 °C, which further emphasizes the inhibitory effect on growth of *E. coli* BL21 at this temperature (Supplementary Figure S10B).

The thermotolerance of *E. coli* cells did not strongly decrease when the endogenous sHSPs were deleted (Figure 7, Supplementary Figure S10). The overexpression of full-length *A*IbpA_{His6} and the N-terminal-truncated *A*IbpAΔN12_{His6} were able to compensate the deficiency of either *Ec*IbpA or both *Ec*IbpAB, but not *Ec*IbpB (Figure 7), suggesting that *A. laidlawii* N-terminus is responsible for the IbpB-like protein functions. Of note, truncated *A*IbpA increased the thermotolerance stronger than the full-length *A*IbpA_{His6}, which could be due to its constitutive fibrillar structure.

Taken together, our data demonstrate non-trivial features of the function and regulation of the chaperone-like activity of sHSP *A*IbpA from *A. laidlawii*. Previously, we reported [48] that the N-terminal domain of *A*IbpA provides the formation of 24-mer

*A*IbpA globules and acts as an autoinhibitor and regulator of the C-terminal domain, which is necessary for the chaperone-like activity and oligomerization of the protein into a fibrillar form. Thus, the effectiveness of the *A. laidlawii* multi-chaperone system seems to be based on the ability of *A*IbpA to form both globular quaternary structures, which are necessary for the sHSP–substrate dissociation as well as on the subsequent protein disaggregation, and fibrils, which, in contrast to *Ec*IbpA, do not inhibit the system *in vivo* (Figure 8). In contrast to *Ec*IbpA and *Ec*IbpB of *Escherichia coli*, which regulate its activity in close cooperation, to the best of our knowledge, *A*IbpA appears the first sHSP, in which the competition between the N- and C-terminal domains regulates the shift of the quaternary structure of the protein into either fibrillar or globular form, thus representing a molecular mechanism of the regulation of its function. Based on our results, we postulate that prior to the final disaggregation process, *A*IbpA can directly transfer the substrate to HSP100, in contrast to the well-described HSP70 from *E. coli*, thereby representing an alternative mechanism in the HSP interaction network.

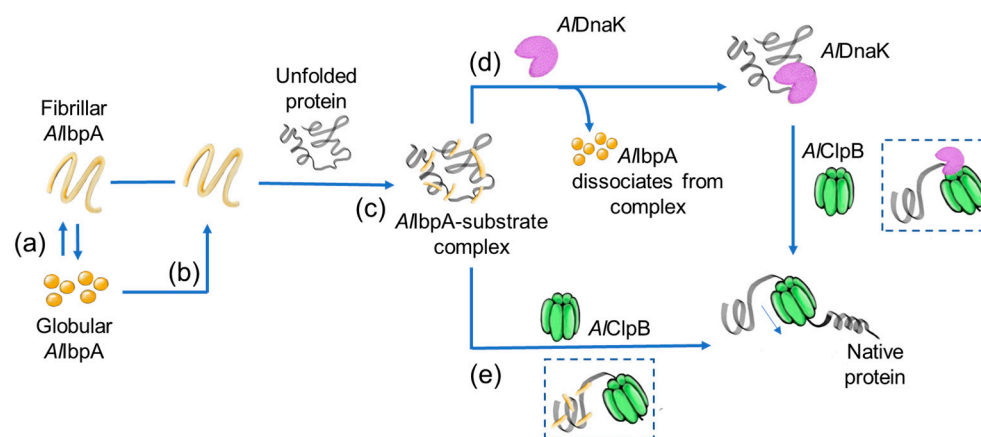


Figure 8. The proposed model of HSP20–HSP70–HSP100-mediated protein disaggregation mechanism in *A. laidlawii*. Inactive *A*IbpA is a heterogeneous mixture of globular and fibrillar oligomers (a). During disaggregation, globular *A*IbpA reorganizes into fibril-like oligomers (b), which efficiently bind proteins with disrupted conformation (c). Stably bound to the substrate, *A*IbpA, in the form of short fibrils (active form of *A*IbpA), is able to dissociate from the *A*IbpA–substrate complex in the presence of *A*DnaK for further refolding of the substrate by the *A*DnaK–*A*ClpB chaperone system (d) or directly transfer the substrate to *A*ClpB (e).

4. Materials and Methods

4.1. Protein Alignment and Structure Analyses

The multiple alignment of amino acid sequences was performed using Clustal Omega web server [55] (accessed on 10 July 2023) and manually refined. The sHSP sequences and models of tertiary structures were obtained using Uniprot servers (accessed on 10 July 2023): *A*IbpA from *Acholeplasma laidlawii* PG-8A WP_012242373.1, *Ec*IbpA from *Escherichia coli* K12 WP_053890241.1 and *Ec*IbpB from *Escherichia coli* K12 NC_000913.3.

4.2. Strains and Plasmids

E. coli XL-10 Gold (Agilent, Santa Clara, CA, USA) was used for cloning procedures. *E. coli* BL21 (Agilent, Santa Clara, CA, USA) and its derivatives were used for protein overexpression and *in vivo* experiments. Primers and plasmids used in this study are listed in Supplementary Tables S1 and S2, respectively. Synthetic genes *dnaK* and *clpB* encoding the HSP70 and HSP100 from *A. laidlawii*, respectively, were synthesized and cloned in pET-28a(+) vector linearized with the restriction endonucleases *Xba*I and *Bam*HI by Synbio Technologies (Monmouth Junction, NJ, USA). The resulting plasmids pET-28a-*A*DnaK_{ST} and pET-28a-*A*ClpB_{ST} provided the IPTG-inducible expression of recombinant C-terminally StrepII-tagged (ST) *A*DnaK and *A*ClpB, respectively, in *E. coli* BL21 cells.

The deletion of HSP genes in *E. coli* BL21 cells was performed accordingly to the protocol described previously by [56]. The *ibpA*, *ibpB* and whole *ibpAB* operon were replaced by a kanamycin resistance cassette; *dnaK* and *clpB* were replaced by spectinomycin and chloramphenicol resistance cassettes, respectively. The deletion schemes are shown in Supplementary Figure S11, and primers are listed in Supplementary Table S1.

4.3. Protein Purification

All recombinant proteins were overexpressed in *E. coli* BL21 (DE3) (Stratagene, La Jolla, CA, USA). The His6-tagged proteins were purified on Ni-NTA agarose (Qiagen, Hilden, Germany), as described in [48]. StrepII-tagged proteins were purified on Strep-tactin agarose (Qiagen, Hilden, Germany), as described in [57]. Detailed description of procedures is given in Supplementary Materials. All proteins were purified to apparent electrophoretic homogeneity, dialyzed against PBS pH 7.4 containing 100 mM NaCl and used immediately for experiments or stored at 4 °C no more than 4 days.

4.4. In Vitro Cross-Linking of Proteins

The chemical cross-linking using glutaraldehyde (GA) was performed as described in [48]. *AllbpA*_{His6} proteins (1.0 mg mL⁻¹) were mixed with human insulin (Sigma-Aldrich, St. Louis, MO, USA) (1.0 mg mL⁻¹), and after 10 min incubation at either 25 °C or 56 °C, the mixture was treated with 0.05% (*v/v*) freshly prepared solution of glutaraldehyde. The reaction was stopped by the addition of 100 mM Tris pH 7.4 after 20 min of incubation.

4.5. Size-Exclusion Chromatography

The analytical size-exclusion chromatography was performed on Superdex 200 10/300 column (Sigma-Aldrich, St. Louis, MO, USA) at flow rate of 0.5 mL min⁻¹ on Waters Breeze 2 equipment with the absorbance detection at 280 nm. The protein sample (1 mg mL⁻¹) was centrifuged for 5 min at 12,000 rpm to remove any sediment, and 100 µL were injected. The running buffer contained 50 mM NaCl, 50 mM KCl and 50 mM K₂HPO₄ pH 7.4. Apparent molecular weights of proteins were estimated after column calibration with blue dextran (2000 kDa), β-amylase (200 kDa), alcohol-dehydrogenase (147 kDa), BSA (66 kDa), papain (23.4 kDa) and lysozyme (14.3 kDa).

4.6. Pull Down Assay

The interaction of purified proteins was assessed on Ni-NTA Sepharose or Strep-Tactin Sepharose (IBA Lifesciences, Göttingen, Germany) on 0.05 mL columns. The purified proteins were mixed in 1:1 (*w/w*), incubated for 1 h at room temperature with shaking in the presence or absence of ligands. Afterwards, 50 µL of resin was added to the samples and incubated for 30 min. Samples were loaded onto columns, washed with 2 mL of His-Wash or Strep-Wash buffer and eluted with 1 mL of His-Elution or Strep-Elution buffer (see Supplementary Materials data for composition). Proteins from the elution fractions were precipitated with trichloroacetic acid and analyzed using SDS-PAGE, followed by silver staining.

To identify potential partner proteins for interaction, the purified recombinant protein was co-eluted with bacterial cell extract on 0.5 mL columns.

A. laidlawii cells were grown in liquid-complete Edwardian nutrient medium (ENM) until early stationary growth phase, harvested by centrifugation, and cell extract was prepared at 30 °C. A total of 1 mg of purified *AllbpA*_{His6} was added to the cell extract, followed by incubation for 1 h at 4 °C, 30 °C, 37 °C or 42 °C. Afterwards, samples were loaded onto columns containing 0.5 mL of Ni-NTA Sepharose, washed with His-Wash buffer and eluted with His-Elution buffer containing 250 mM imidazole. The eluate was harvested, precipitated with trichloroacetic acid and analyzed using SDS-PAGE, and co-eluted proteins were identified using LC-MS on Maxis Impact (Bruker, Billerica, MA, USA).

4.7. Transmission Electron Microscopy

The samples of either full-length *A//bpA*_{His6} or *A//bpAN12*_{His6} proteins (cross-linked alone or in presence of substrate proteins) were negatively stained on grids as described in [48]. Briefly, nickel grids (400 mesh, Electron Microscopy Sciences, Hatfield, PA, USA) were treated with 2% collodion solution for film formation. Right before the experiment, grids were discharged using UV during 1 min, followed by immediate addition of 5 μ L protein solution for 15 s and its further removal with filter paper. This step was followed by the addition of 4 μ L Uranyl Acetate Alternative (Ted Pella, Redding, CA, USA) for 15 s, after which the contrast agent was also removed with filter paper. Samples were visualized on a Libra 120 electron microscope (Zeiss, Oberkochen, Germany) at 10,000–20,000 magnification. The quantification of aggregate sizes was performed using in-house developed software [57].

4.8. Bio-Layer Interferometry

The bio-layer interferometry experiments were performed on the BLItz platform (FortéBio, Fremont, CA, USA) using high-precision streptavidin (SAX) biosensors (FortéBio, Fremont, CA, USA). The protocol provided by BLItz Pro software in the Advanced Kinetics module was modified, as indicated in Supplementary Table S3.

Biosensors preparation. Proteins for immobilization were biotinylated using EZ-Link NHS-PEG4-biotin (Thermo Fisher Scientific, Waltham, MA, USA), as recommended by manufacturer. Briefly, protein solution (10 μ M in PBS) was mixed with biotin solution (10 μ M in PBS) and incubated for 30 min at room temperature. Free biotin was removed using zebra spin desalting spin columns (3 kDa MWCO) (Thermo Fisher Scientific, Waltham, MA, USA). The streptavidin K biosensors were hydrated in PBS buffer pH 7.4 for 10 min and then loaded into biotinylated protein solution (10 μ M) for 120 s. Finally, 2.0 nm protein layer was loaded, and the biosensor was washed with PBS pH 7.4 for 30 s.

Measurements. The binding assay was started using equilibration of a prepared biosensor in PBS pH 7.4 for 30 s (baseline). Next, the sensor was loaded into analyte protein solution (10 μ M) for 300 s for association and then placed back into PBS for 300 s for dissociation. The biosensors were stored in PBS between measurements. Between samples, the drop holder was washed with 0.1 M HCl, twice-rinsed with pure water and dried with precision wipes (Kimberly Clark, Irving, TX, USA). A 10 μ M BSA solution served as negative binding control and was subtracted from the experimental binding data (control curve shown in Supplementary Figure S12). K_D values were calculated based on binding-dissociation curves using BLItz Pro data analysis software (version: 1.3.0.5). For each interaction pair, the procedure was repeated at least 6 times in increasing concentrations until the K_D value became stable and values were averaged.

4.9. In Vitro Chaperone-like Activity Assay

The chaperone-like activity was investigated by measuring the capacity of *A//bpA* to suppress the heat shock-induced aggregation of human insulin (Sigma-Aldrich, St. Louis, MO, USA). The protein aggregation was assessed by measuring the fluorescence of SYPRO Orange, as described in [48]. Briefly, the human insulin (0.1 mg) was mixed with either full-length *A//bpA*_{His6} or *A//bpAN12*_{His6} proteins (0.1 mg) in total volume of 30 μ L and heated from 10 °C to 95 °C with a temperature increment of 1 °C per 1 min in PBS containing 10 μ M SYPRO Orange (Sigma-Aldrich, St. Louis, MO, USA). The fluorescence was measured with excitation at 492 nm and emission at 516 nm on Bio-Rad CFX96 thermocycler [55]. The data were presented as the temperature leading to maximal increase in fluorescent signal (T_m 100).

4.10. Cell Viability Test

The overnight cultures of recombinant *E. coli* strains were diluted in fresh LB medium (1:100) and grown at 37 °C on a shaker at 180 rpm until $OD_{600} = 0.6$. After 1 h incubation at 30 °C with IPTG (1 mM) to allow proteins expression, the cells were subjected to heat stress

(56 °C) for 1 h. Subsequently, 100 µL of yellow tetrazolium salt (3-(4,5-dimethylthiazol-2-yl)-2,5-diphenyltetrazolium bromide, MTT) (Sigma-Aldrich, St. Louis, MO, USA) was added to 100 µL of cell suspension and incubated for 5–10 min at 30 °C. Afterwards, the plates were centrifuged for 5 min at 3500 rpm, supernatant was discarded and 200 µL of DMSO (Merck, Darmstadt, Germany) was added to the sediment to solubilize formazan crystals. The absorbance was measured on a Tecan infinite 200 Pro microplate reader (Tecan, Männedorf, Switzerland) at 550 nm. The viability of cells was calculated in percentage of residual metabolic activity considering the activity before heat treatment as 100%.

4.11. Statistical Analyses

All experiments were performed in biological triplicates with three repeats in each run. The data were analyzed and graphically visualized using GraphPad Prism version 6.00 for Windows (GraphPad Software, Boston, MA, USA, <https://www.graphpad.com>, accessed on 1 March 2015). The comparison with the control was performed using the non-parametric Kruskal–Wallis test. Significant differences were considered at $p < 0.05$. The elution profiles were analyzed using Waters Breeze 2 software.

Supplementary Materials: The supporting information can be downloaded at: <https://www.mdpi.com/article/10.3390/ijms242015445/s1>. References [58,59] are cited in the supplementary materials.

Author Contributions: Conceptualization, L.S.C. and A.R.K.; methodology, A.R.K., I.E.V., J.B. and K.M.T.; software, M.I.B.; validation, L.S.C., A.R.K. and I.E.V.; formal analysis, I.E.V.; investigation, L.S.C. and I.E.V.; resources, A.R.K., I.E.V. and K.M.T.; data curation, M.I.B.; writing—original draft preparation, L.S.C. and A.R.K.; writing—review and editing, A.R.K., L.S.C., J.B., I.E.V. and M.I.B.; visualization, L.S.C., A.R.K. and I.E.V.; supervision, A.R.K. and I.E.V.; project administration, A.R.K. and I.E.V.; funding acquisition, A.R.K. and I.E.V. Manuscript ideas and editing of relevant sections by all authors. All authors have read and agreed to the published version of the manuscript.

Funding: This research was funded by the Russian Science Foundation, grant number 22-24-01150.

Institutional Review Board Statement: Not applicable.

Informed Consent Statement: Not applicable.

Data Availability Statement: The data analyzed during the current study are available from the corresponding author upon request.

Acknowledgments: This work was part of the Kazan Federal University Strategic Academic Leadership Program (PRIORITY-2030).

Conflicts of Interest: The authors declare that the research was conducted in the absence of any commercial or financial relationships that could be construed as potential conflict of interest.

References

1. Dubrez, L.; Causse, S.; Borges Bonan, N.; Dumétier, B.; Garrido, C. Heat-shock proteins: Chaperoning DNA repair. *Oncogene* **2020**, *39*, 516–529. [[CrossRef](#)] [[PubMed](#)]
2. Jee, H. Size dependent classification of heat shock proteins: A mini-review. *J. Exerc. Rehabil.* **2016**, *12*, 255–259. [[CrossRef](#)]
3. Liberek, K.; Lewandowska, A.; Zietkiewicz, S. Chaperones in control of protein disaggregation. *EMBO J.* **2008**, *27*, 328–335. [[CrossRef](#)] [[PubMed](#)]
4. Mogk, A.; Deuerling, E.; Vorderwülbecke, S.; Vierling, E.; Bukau, B. Small heat shock proteins, ClpB and the DnaK system form a functional triade in reversing protein aggregation. *Mol. Microbiol.* **2003**, *50*, 585–595. [[CrossRef](#)]
5. Ul Haq, S.; Khan, A.; Ali, M.; Khattak, A.M.; Gai, W.-X.; Zhang, H.-X.; Wei, A.-M.; Gong, Z.-H. Heat shock proteins: Dynamic biomolecules to counter plant biotic and abiotic stresses. *Int. J. Mol. Sci.* **2019**, *20*, 5321. [[CrossRef](#)]
6. Ehrnsperger, M.; Hergersberg, C.; Wienhues, U.; Nichtl, A.; Buchner, J. Stabilization of proteins and peptides in diagnostic immunological assays by the molecular chaperone Hsp25. *Anal. Biochem.* **1998**, *259*, 218–225. [[CrossRef](#)] [[PubMed](#)]
7. Mogk, A.; Bukau, B. Role of sHsps in organizing cytosolic protein aggregation and disaggregation. *Cell Stress Chaperones* **2017**, *22*, 493–502. [[CrossRef](#)]
8. De Graff, A.M.; Mosedale, D.E.; Sharp, T.; Dill, K.A.; Grainger, D.J. Proteostasis is adaptive: Balancing chaperone holdases against foldases. *PLoS Comput. Biol.* **2020**, *16*, e1008460. [[CrossRef](#)]
9. Bandyopadhyay, B.; Das Gupta, T.; Roy, D.; Das Gupta, S.K. DnaK dependence of the mycobacterial stress-responsive regulator HspR is mediated through its hydrophobic C-terminal tail. *J. Bacteriol.* **2012**, *194*, 4688–4697. [[CrossRef](#)]

10. Raman, S.; Song, T.; Puyang, X.; Bardarov, S.; Jacobs, W.R.; Husson, R.N. The alternative sigma factor SigH regulates major components of oxidative and heat stress responses in *Mycobacterium tuberculosis*. *J. Bacteriol.* **2001**, *183*, 6119–6125. [[CrossRef](#)]
11. Ullers, R.S.; Luirink, J.; Harms, N.; Schwager, F.; Georgopoulos, C.; Genevaux, P. SecB is a *bona fide* generalized chaperone in *Escherichia coli*. *Proc. Natl. Acad. Sci. USA* **2004**, *101*, 7583–7588. [[CrossRef](#)] [[PubMed](#)]
12. Vorderwülbecke, S.; Kramer, G.; Merz, F.; Kurz, T.A.; Rauch, T.; Zachmann-Brand, B.; Bukau, B.; Deuerling, E. Low temperature of GroEL/ES overproduction permits growth of *Escherichia coli* cells lacking trigger factor DnaK. *FEBS Lett.* **2005**, *579*, 181–187. [[CrossRef](#)]
13. Målen, H.; Berven, F.S.; Fladmark, K.E.; Wiker, H.G. Comprehensive analysis of exported proteins from *Mycobacterium tuberculosis* H37Rv. *Proteomics* **2007**, *7*, 1702–1718. [[CrossRef](#)] [[PubMed](#)]
14. Stewart, G.R.; Snewin, V.A.; Walzl, G.; Hussell, T.; Tormay, P.; O’Gaora, P.; Goyal, M.; Betts, J.; Brown, I.N.; Young, D.B. Overexpression of heat-shock proteins reduces survival of *Mycobacterium tuberculosis* in the chronic phase of infection. *Nat. Med.* **2001**, *7*, 732–737. [[CrossRef](#)] [[PubMed](#)]
15. Franck, E.; Madsen, O.; van Rheede, T.; Ricard, G.; Huynen, M.A.; de Jong, W.W. Evolutionary diversity of vertebrate small heat shock proteins. *J. Mol. Evol.* **2004**, *59*, 792–805. [[CrossRef](#)] [[PubMed](#)]
16. Basha, E.; O’Neill, H.; Vierling, E. Small heat shock proteins and α -crystallins: Dynamic proteins with flexible functions. *Trends Biochem. Sci.* **2012**, *37*, 106–117. [[CrossRef](#)]
17. Lindner, R.A.; Carver, J.A.; Ehrnsperger, M.; Buchner, J.; Esposito, G.; Behlke, J.; Lutsch, G.; Kotlyarov, A.; Gaestel, M. Mouse Hsp25, a small shock protein. The role of its C-terminal extension in oligomerization and chaperone action. *Eur. J. Biochem.* **2000**, *267*, 1923–1932. [[CrossRef](#)]
18. Stróżecka, J.; Chrusciel, E.; Górna, E.; Szymanska, A.; Ziętkiewicz, S.; Liberek, K. Importance of N- and C-terminal regions of IbpA, *Escherichia coli* small heat shock protein, for chaperone function and oligomerization. *J. Biol. Chem.* **2012**, *287*, 2843–2853. [[CrossRef](#)]
19. Sun, Y.; MacRae, T.H. Small heat shock proteins: Molecular structure and chaperone function. *Cell Mol. Life Sci.* **2005**, *62*, 2460–2476. [[CrossRef](#)] [[PubMed](#)]
20. Bhandari, V.; Houry, W.A. Substrate interaction networks of the *Escherichia coli* chaperones: Trigger factor, DnaK and GroEL. *Adv. Exp. Med. Biol.* **2015**, *883*, 271–294. [[CrossRef](#)]
21. Clerico, E.M.; Tiliitsky, J.M.; Meng, W.; Gierasch, L.M. How hsp70 molecular machines interact with their substrates to mediate diverse physiological functions. *J. Mol. Biol.* **2015**, *427*, 1575–1588. [[CrossRef](#)] [[PubMed](#)]
22. Mayer, M.P.; Bukau, B. Hsp70 chaperones: Cellular functions and molecular mechanism. *Cell Mol. Life Sci.* **2005**, *62*, 670–684. [[CrossRef](#)] [[PubMed](#)]
23. Mayer, M.P.; Gierasch, L.M. Correction: Recent advances in the structural and mechanistic aspects of Hsp70 molecular chaperones. *J. Biol. Chem.* **2020**, *295*, 288. [[CrossRef](#)]
24. Kravats, A.N.; Doyle, S.M.; Hoskins, J.R.; Genest, O.; Doody, E.; Wickner, S. Interaction of *E. coli* Hsp90 with DnaK Involves the DnaJ Binding Region of DnaK. *J. Mol. Biol.* **2017**, *429*, 858–872. [[CrossRef](#)]
25. Mayer, M.P. Hsp70 chaperone dynamics and molecular mechanism. *Trends Biochem. Sci.* **2013**, *38*, 507–514. [[CrossRef](#)]
26. Rüdiger, S.; Buchberger, A.; Bukau, B. Interaction of Hsp70 chaperones with substrates. *Nat. Struct. Biol.* **1997**, *4*, 342–349. [[CrossRef](#)]
27. Rosenzweig, R.; Farber, P.; Velyvis, A.; Rennella, E.; Latham, M.P.; Kay, L.E. ClpB N-terminal domain plays a regulatory role in protein disaggregation. *Proc. Natl. Acad. Sci. USA* **2015**, *112*, E6872–E6881. [[CrossRef](#)]
28. Squires, C.L.; Pedersen, S.; Ross, B.M.; Squires, C. ClpB is the *Escherichia coli* heat shock protein F84.1. *J. Bacteriol.* **1991**, *173*, 4254–4262. [[CrossRef](#)]
29. Goloubinoff, P.; Mogk, A.; Zvi, A.P.; Tomoyasu, T.; Bukau, B. Sequential mechanism of solubilization and refolding of stable protein aggregates by a bichaperone network. *Proc. Natl. Acad. Sci. USA* **1999**, *96*, 13732–13737. [[CrossRef](#)]
30. Hanson, P.I.; Whiteheart, S.W. AAA+ proteins: Have engine, will work. *Nat. Rev. Mol. Cell Biol.* **2005**, *6*, 519–529. [[CrossRef](#)] [[PubMed](#)]
31. Hodson, S.; Marshall, J.J.T.; Burston, S.G. Mapping the road to recovery: The ClpB/Hsp104 molecular chaperone. *J. Struct. Biol.* **2012**, *179*, 161–171. [[CrossRef](#)]
32. Neuwald, A.F.; Aravind, L.; Spouge, J.L.; Koonin, E.V. AAA+: A Class of Chaperone-Like ATPases Associated with the Assembly, Operation, and Disassembly of Protein Complexes. *Genome Res.* **1999**, *9*, 27–43. [[CrossRef](#)] [[PubMed](#)]
33. Zolkiewski, M. ClpB cooperates with DnaK, DnaJ, and GrpE in suppressing protein aggregation. A novel multi-chaperone system from *Escherichia coli*. *J. Biol. Chem.* **1999**, *274*, 28083–28086. [[CrossRef](#)] [[PubMed](#)]
34. Zolkiewski, M.; Zhang, T.; Nagy, M. Aggregate reactivation mediated by the Hsp100 chaperones. *Arch. Biochem. Biophys.* **2012**, *520*, 1–6. [[CrossRef](#)]
35. Saibil, H. Chaperone machines for protein folding, unfolding and disaggregation. *Nat. Rev. Mol. Cell Biol.* **2013**, *14*, 630–642. [[CrossRef](#)]
36. Doyle, S.M.; Shorter, J.; Zolkiewski, M.; Hoskins, J.R.; Lindquist, S.; Wickner, S. Asymmetric deceleration of ClpB or Hsp104 ATPase activity unleashes protein-remodeling activity. *Nat. Struct. Mol. Biol.* **2007**, *14*, 114–122. [[CrossRef](#)]
37. Zhang, T.; Kedzierska-Mieszkowska, S.; Liu, H.; Cheng, C.; Ganta, R.R.; Zolkiewski, M. Aggregate-reactivation activity of the molecular chaperone ClpB from *Ehrlichia chaffeensis*. *PLoS ONE* **2013**, *8*, e62454. [[CrossRef](#)]

38. Miot, M.; Reidy, M.; Doyle, S.M.; Hoskins, J.R.; Johnston, D.M.; Genest, O.; Vitery, M.-C.; Masison, D.C.; Wickner, S. Species-specific collaboration of heat shock proteins (Hsp) 70 and 100 in thermotolerance and protein disaggregation. *Proc. Natl. Acad. Sci. USA* **2011**, *108*, 6915–6920. [[CrossRef](#)] [[PubMed](#)]
39. Schlee, S.; Beinker, P.; Akhrymuk, A.; Reinstein, J. A chaperone network for the resolubilization of protein aggregates: Direct interaction of ClpB and DnaK. *J. Mol. Biol.* **2004**, *336*, 275–285. [[CrossRef](#)]
40. Obuchowski, I.; Piróg, A.; Stolarska, M.; Tomiczek, B.; Liberek, K. Duplicate divergence of two bacterial small heat shock proteins reduces the demand for Hsp70 in refolding of substrates. *PLoS Genet.* **2019**, *15*, e1008479. [[CrossRef](#)]
41. Ratajczak, E.; Zietkiewicz, S.; Liberek, K. Distinct activities of *Escherichia coli* small heat shock proteins IbpA and IbpB promote efficient protein disaggregation. *J. Mol. Biol.* **2009**, *386*, 178–189. [[CrossRef](#)]
42. Bissonnette, S.A.; Rivera-Rivera, I.; Sauer, R.T.; Baker, T.A. The IbpA and IbpB small heat-shock proteins are substrates of the AAA+ Lon protease. *Mol. Microbiol.* **2010**, *75*, 1539–1549. [[CrossRef](#)]
43. Haslbeck, M.; Vierling, E. A first line of stress defense: Small heat shock proteins and their function in protein homeostasis. *J. Mol. Biol.* **2015**, *427*, 1537–1548. [[CrossRef](#)] [[PubMed](#)]
44. Mogk, A.; Ruger-Herreros, C.; Bukau, B. Cellular functions and mechanisms of action of small heat shock proteins. *Annu. Rev. Microbiol.* **2019**, *73*, 89–110. [[CrossRef](#)]
45. Zwirowski, S.; Kłosowska, A.; Obuchowski, I.; Nillegoda, N.B.; Piróg, A.; Zietkiewicz, S.; Bukau, B.; Mogk, A.; Liberek, K. Hsp70 displaces small heat shock proteins from aggregates to initiate protein refolding. *EMBO J.* **2017**, *36*, 783–796. [[CrossRef](#)]
46. Vishnyakov, I.E.; Borchsenius, S.N. *Mycoplasma* heat shock proteins and their genes. *Microbiology* **2013**, *82*, 643–659. [[CrossRef](#)]
47. Vishnyakov, I.E.; Levitskii, S.A.; Manuvera, V.A.; Lazarev, V.N.; Ayala, J.A.; Ivanov, V.A.; Snigirevskaya, E.S.; Komissarchik, Y.Y.; Borchsenius, S.N. The identification and characterization of IbpA, a novel α -crystallin-type heat shock protein from mycoplasma. *Cell Stress Chaperones* **2012**, *17*, 171–180. [[CrossRef](#)] [[PubMed](#)]
48. Chernova, L.S.; Bogachev, M.I.; Chasov, V.V.; Vishnyakov, I.E.; Kayumov, A.R. N- and C-terminal regions of the small heat shock protein IbpA from *Acholeplasma laidlawii* competitively govern its oligomerization pattern and chaperone-like activity. *RSC Adv.* **2020**, *10*, 8364–8376. [[CrossRef](#)] [[PubMed](#)]
49. Bukach, O.V.; Seit-Nebi, A.S.; Marston, S.B.; Gusev, N.B. Some properties of human small heat shock protein Hsp20 (HspB6). *Eur. J. Biochem.* **2004**, *271*, 291–302. [[CrossRef](#)]
50. Horwitz, J.; Huang, Q.L.; Ding, L.; Bova, M.P. Lens α -crystallin: Chaperone-like properties. *Methods Enzymol.* **1998**, *290*, 365–383. [[CrossRef](#)] [[PubMed](#)]
51. Sharma, K.K.; Kumar, R.S.; Kumar, G.S.; Quinn, P.T. Synthesis and characterization of a peptide identified as a functional element in α A-crystallin. *J. Biol. Chem.* **2000**, *275*, 3767–3771. [[CrossRef](#)] [[PubMed](#)]
52. Haslbeck, M.; Weinkauff, S.; Buchner, J. Small heat shock proteins: Simplicity meets complexity. *J. Biol. Chem.* **2019**, *294*, 2121–2132. [[CrossRef](#)]
53. Ratajczak, E.; Stróżecka, J.; Matuszewska, M.; Zietkiewicz, S.; Kuczyńska-Wiśnik, D.; Laskowska, E.; Liberek, K. IbpA the small heat shock protein from *Escherichia coli* forms fibrils in the absence of its cochaperone IbpB. *FEBS Lett.* **2010**, *584*, 2253–2257. [[CrossRef](#)]
54. Kitagawa, M.; Matsumura, Y.; Tsuchido, T. Small heat shock proteins, IbpA and IbpB, are involved in resistances to heat and superoxide stresses in *Escherichia coli*. *FEMS Microbiol. Lett.* **2000**, *184*, 165–171. [[CrossRef](#)] [[PubMed](#)]
55. Armenta, S.; Sánchez-Cuapio, Z.; Farrés, A.; Manoutcharian, K.; Hernandez-Santoyo, A.; Sánchez, S.; Rodríguez-Sanoja, R. Data concerning secondary structure and alpha-glucans-binding capacity of the LaCBM26. *Data Brief.* **2018**, *21*, 1944–1949. [[CrossRef](#)]
56. Edelmann, D.; Berghoff, B.A. Type I toxin-dependent generation of superoxide affects the persisters life cycle of *Escherichia coli*. *Sci. Rep.* **2019**, *9*, 14256. [[CrossRef](#)] [[PubMed](#)]
57. Hauf, K.; Kayumov, A.; Gloge, F.; Forchhammer, K. The molecular basis of trna control by glutamine synthetase in *Bacillus subtilis*. *J. Biol. Chem.* **2016**, *291*, 3483–3495. [[CrossRef](#)]
58. Guérout-Fleury, A.M.; Frandsen, N.; Stragier, P. Plasmids for ectopic integration in *Bacillus subtilis*. *Gene* **1996**, *180*, 57–61. [[CrossRef](#)] [[PubMed](#)]
59. Datta, S.; Costantino, N.; Court, D.L. A set of recombineering plasmids for gram-negative bacteria. *Gene* **2006**, *379*, 109–115. [[CrossRef](#)] [[PubMed](#)]

Disclaimer/Publisher's Note: The statements, opinions and data contained in all publications are solely those of the individual author(s) and contributor(s) and not of MDPI and/or the editor(s). MDPI and/or the editor(s) disclaim responsibility for any injury to people or property resulting from any ideas, methods, instructions or products referred to in the content.